Available online at www.sciencedirect.com

SciVerse ScienceDirect

Physics Procedia 39 (2012) 416 – 424

Physics Procedia

LANE 2012

Material properties of Ti6Al4V parts produced by laser metal deposition

Jun Yu*, Marleen Rombouts, Gert Maes, Filip Motmans

VITO (Flemish Institute for Technological Research), Materials Technology, Boeretang 200, 2400 Mol, Belgium

Abstract

This paper presents our recent progress on the applications of laser metal deposited (LMD) Ti6Al4V parts. The microstructure of the fabricated parts shows prior columnar β grains consisting of acicular α' martensite. The yield and ultimate tensile strengths of the fabricated parts are superior to those of cast and annealed wrought material, while the elongation is lower. On-line monitoring and control of the LMD process was performed by monitoring the pool area and feedback controlling the laser power in order to decrease heat accumulation. The substrate dilution is diminished and the decreased heat accumulation reduces its effects on the microstructure.

Keywords: laser metal depostion; titanium alloy; oxygen content; monitoring and control

1. Motivation / State of the Art

Laser metal deposition (LMD) – also called laser engineering net shape (LENS), direct metal deposition (DMD) or laser solid forming (LSF) – is a process that has a unique capability to build up complex three dimensional features in an additive way on existing components. During this process, a laser source is used to melt metal-based powders delivered in a transport gas stream by means of a coaxial nozzle on to a metal substrate. A shielding gas stream is applied to constraint the powder stream and gives a primary protection from the atmosphere to the melt pool.

The main application area in industry for LMD technology is to build up or to repair high-value components. In these cases, titanium alloys play an important role, such as in building up titanium rudders or repairing titanium turbine blades. Ti6Al4V alloy, a α/β titanium alloy with high strength, low weight ratio and outstanding corrosion resistance, has a large number of applications in aerospace and

* Corresponding author. Tel.: +32-14-335696 ; fax: +32-14-321186 .
E-mail address: : jun.yu@vito.be .

1875-3892 doi:10.1016/j.phpro.2012.10.056

automotive as well as in surgery, medicine, chemical plants, power generation, oil and gas extraction, sports,… [1-3]. LMD of near-net-shape Ti6Al4V components using the solid freeform fabrication route has capacity to meet the requirements of low cost, short cycle and high performance for the production and repair of complex shaped parts.

The background of this paper is using titanium alloy Ti6Al4V powder to produce functional components directly or to build up functional structures on existing parts. In this case, the knowledge of the bulk mechanical properties of the LMD material is really important. The microstructure of these components differs substantially from conventional material due to the rapid solidification, which results in a fine grain-sized microstructure. Although these microstructural features often bring out improvements in properties, rapidly solidified microstructures in commercial alloys that were designed to be used in conventionally processed condition do not necessarily show superior properties [4].

This paper shows the present research progress on LMD Ti6Al4V parts. The titanium alloy Ti6Al4V parts were built without the use of an inert gas chamber but with local protection using an argon gas flow provided by the powder nozzle. Their oxygen content was measured after LMD process and the microstructure, the mechanical properties of the built parts are presented too. A monitoring and control system is adopted to on-line monitor the process and assure the parts' quality by controlling the laser power on-line. Its effects on dilution and heat accumulation are presented as well. Some related works, like titanium parts built in the glove box as well as with heat treatment, are ongoing and will be presented in the near future.

2. Experiment

The experiments were carried out using a 7 kW IPG fiber laser with out-coupling fiber with a diameter of 600 μm. The use of a focal lens with a focal length of 250 mm and a collimator lens with a focal length of 125 mm results in a laser spot diameter of 1200 μm on the substrate. The laser spot has a top-hat energy distribution and the powder was transported through a coaxial nozzle (Fraunhofer-Institut für Lasertechnik) continuously with argon shielding gas stream (the shielding gas flow rate shown in Table 1 represented as *Qs*). Specimens were built on Ti6Al4V flat substrates with a thickness of 10 mm. In addition, SKM-DCAM software is used for generating CNC program with specified tool paths.

In order to fabricate parts with good dimensional and shape accuracy, for each layer, the powders were deposited firstly along the contour and then the interior along raster deposition pattern that was rotated 90 degree between each layer. There was a 0.3 mm overlap between raster and contour paths and 0.6mm (50%) overlap between raster paths. Table 1 shows the experimental processing parameters, in which, *P*, *V*, *D*, *F* , η , *Qs* and *hc* are the laser power, scan speed, spot diameter, powder feed rate, overlap, shield gas flow rate and layer thickness, respectively. The chemical compositions of titanium alloy Ti6Al4V from the supplier are shown in Table 2.

Table 1. Experimental processing parameters in present study

Para. Sets	*P* (W)	*V* (mm/min)	*D* (mm)	*F* (g/min)	η	*Qs* (L/min)	*hc* (mm)
1	380	1000	1,2	1,43	50%	10,5	0,4
2	470	1000	1,2	1,43	50%	10,5	0,5
3	570	1000	1,2	1,43	50%	10,5	0,5
4	520	1500	1,2	1,98	50%	10,5	0,5
5	570	1500	1,2	1,98	50%	10,5	0,5

Table 2. Chemical compositions of titanium alloy Ti6Al4V from supplier (wt%)

Al	V	C	Fe	O	N	H	Ti
0,019	0,006	0,017	0,53	0,092	0,010	0,004	Bal.

The microstructure was studied by optical microscopy and X-ray Diffraction (Siemens D500). The specimens were etched using a solution of hydrochloride acid, nitric acid and hydrofluoric acid. The hardness was obtained by Vickers indentation measurements using a load of 1 kg. The mechanical properties were determined by tensile testing (Instron 5582) using an extensometer according to ASTM E-8M standard. Three parts produced under identical conditions have been subjected to tensile testing shown in Fig. 1(a), in which, the image of the milled part is also illustrated. These parts are 20*100 mm² and 10 mm high and then are milled to the final dimension (see Fig. 1(b)) prior to tensile testing.

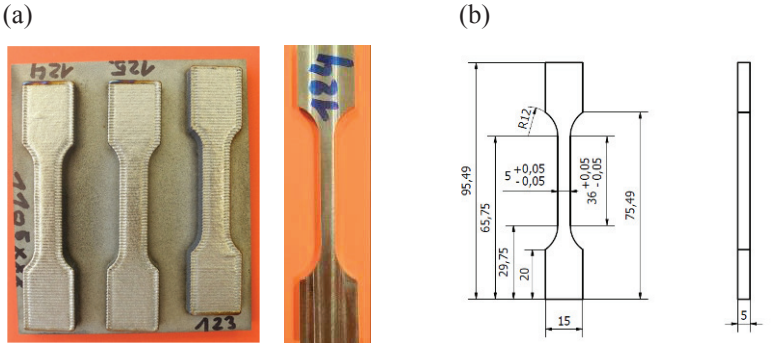

Fig. 1. Tensile test (a) specimens including a representative of the milled parts; (b) dimensions (in mm) of the milled par

A melt pool based monitoring and control system (Fraunhofer IWS, Dresden) constituting of a CCD camera (E-MAqS) for monitoring the melt pool area and a laser process control system (LompocPro) for real-time control of the laser power has been applied. Preliminary experiments encompassing laser cladding of single lines, layers and 3D parts have been carried out.

3. Results and Discussion

Figure 2(a) shows the particle morphology for the Ti6Al4V powder. The particle size is around 30~80 μm and some pores are occasionally present in the particles. Figures 2(b)~(d) show cross-section of three fabricated specimens with a dimension of 15*10*5 mm^3 using the processing parameters sets 1-3 in Table 1, respectively. Pores and bad-bonding defects can only be found when using the lowest laser power 380W, i.e. set 1 in Table 1 (big magnification, area 1).

The macrostructure shows prior columnar β grains which are oriented more or less in the building direction, as shown in Fig. 3(a)~(c). The prior β grains grow epitaxially and get a little coarser with the laser power increase. The microstructure is composed of acicular α'-martensite as shown in Fig. 4. This can be proved by the evidence mentioned in the literature [5] comparing the hcp lattice parameters. In present study, the measured lattice parameters are a=0.293 nm and c=0.467 nm determined by X-ray diffraction, which correspond well to the lattice parameter values given in the literature [6] for the α' phase, i.e. a=0.29313 nm and c= 0.46813 nm. In addition, Murr et al. [7-9] and Koike et al. [10] have

demonstrated that selective laser melting (SLM)/laser beam melting (LBM) fabrication of Ti6Al4V components exhibits α' martensitic or α'/α microstructures in contrast to primarily α/β microstructures for electron beam melting (EBM) fabricated Ti6Al4V components because during LBM a higher cooling rate is imposed on the material than during EBM. The α' phase is beneficially produced by the rapid cooling through diffusionless transformation. In fact, the cooling rate during LMD is around 10^6 °C/min at the current process parameters. This is even much higher than the cooling rate of water quenching which is around 10^5 °C /min [11] and in general produces α' martensitic microstructure [12-14].

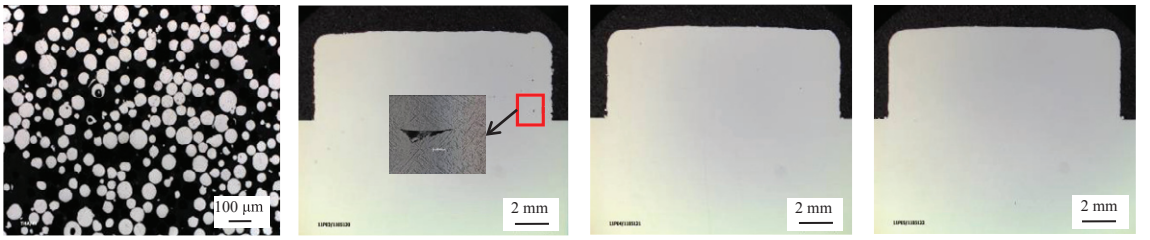

Fig. 2. Particle morphology ancross-sections of the specimens (a) Ti6Al4V particles and cross-sections of Ti6Al4V specimen using parameter (b) set 1, (c) set 2 and (d) set 3 in Table 1

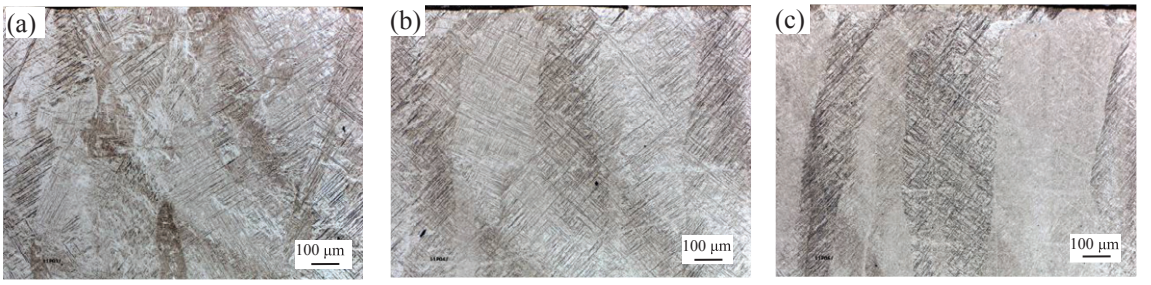

Fig. 3. Macrostructures of LMD Ti6Al4V specimens using different parameter sets; (a) parameter set 1; (b) parameter set 2; (c) parameter set 3 in Table 1

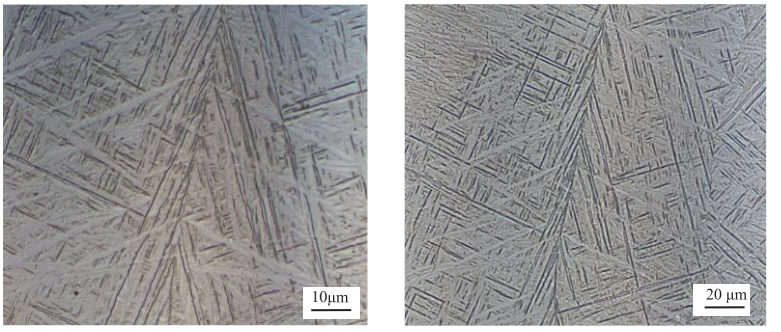

Fig. 4. Microstructures of LMD Ti6Al4V specimen using parameter set 1 in Table 1 (big magnification of Fig. 3 (a))

Figure 5 shows the hardness test results for the specimens in Fig. 2(b)~(d) including the testing positions as well. The points 1-10 in Fig. 5(a) are located on the substrate (Ti6Al4V) and the others are on the fabricated specimen. The hardness of the fabricated specimen is around 360 ±10 HV and higher than the forging substrate plate. The laser power didn't have significant influence on the hardness of the fabricated specimens under current experimental conditions with the laser power being changed from 380 W to 570 W.

Laser metal deposition can produce high melt pool temperature and much heat accumulation leading to bad oxidation of the fabricated parts at high heat inputs. Hence, the parameter set 2 with laser power 470W was adopted to fabricate tensile test parts, taking into account the protection of the parts against oxidation as much as possible. In this case, three tensile test parts were fabricated under identical conditions (see Fig. 1(a)). The density of these three parts was measured using Archimedes method. The results are 4.421g/cm^3, 4.417g/cm^3 and 4.419g/cm^3, respectively and in average, the relative density can be up to 99.8%. One of these parts was tested for oxygen level using instrumental gas analysis (IGA). The result was 0.13 wt% and shows a 0.038 wt% increase comparing with of the powder.

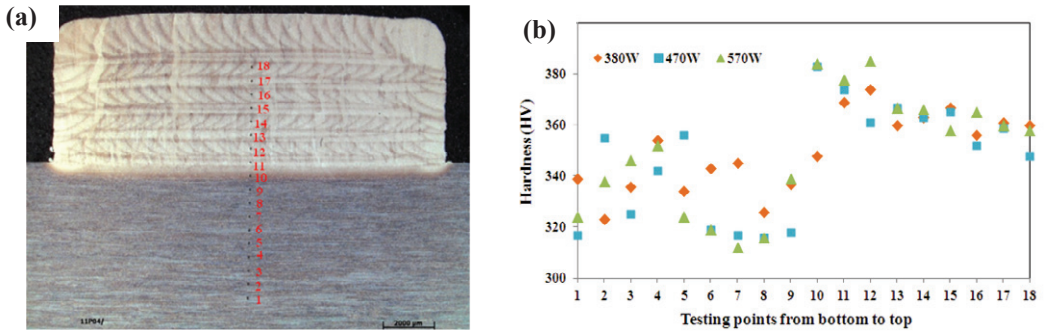

Fig. 5. Hardness test for Ti6Al4V specimens (a) the test points (b) hardness with the use of different laser powers

The mechanical property results of the fabricated parts are shown in Fig. 6 with respect to yield strength, ultimate tensile strength (Fig. 6(a)) and elongation (Fig. 6(b)). As a reference, the data for cast [15] and annealed wrought material were introduced [16]. The yield and ultimate tensile strengths of the three LMD parts are 976 ± 24 MPa and 1099 ± 2 MPa, respectively, which are higher than for cast and annealed wrought material. The elongation is 4.9 ± 0.1. It is reported that oxygen is detrimental to the ductility through producing interstitial solid solution with Ti at high temperature [17, 18]. Better oxygen control during build-up is good for improving the elongation property (up to 13%) [19]. Besides, the elongation to failure is strongly dependent on the present microstructure, therefore, another effective way is reforming the microstructure by heat treatment (up to 14%) [12] because the α' martensite microstructure itself shows a low ductility.

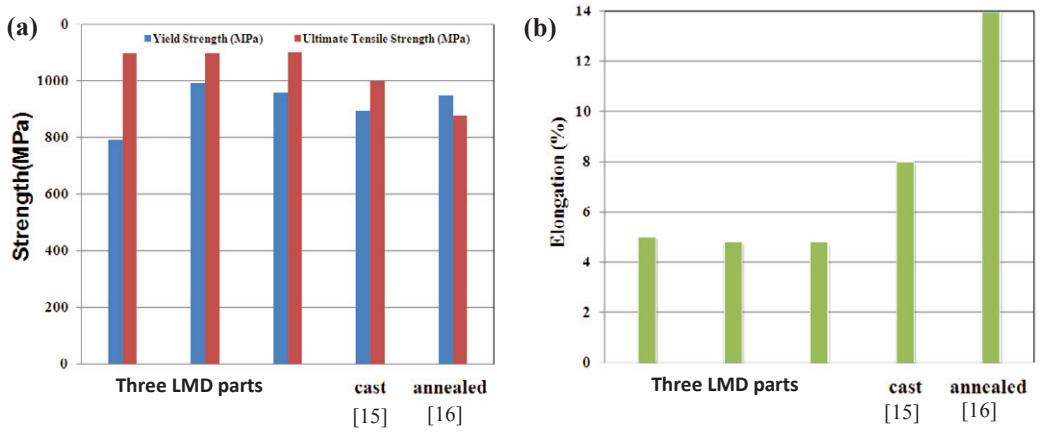

Fig. 6. Tensile test results of the Ti6Al4V specimens (a) Yield and Ultimate tensile strengths (b) Elongation

Heat accumulation is inevitable during LMD process and will get increased layer by layer, which can lead to an increasing pool spreading behavior [20], a high oxidation level and a big heat distortion [21] producing bad deposition shape or accuracy of the built parts. It can also lead to the coarsening of the microstructure due to the increasing temperature and the decreasing cooling rate of melt pool. In order to decrease the accumulated heat compared with the use of a constant heat input, the monitoring and control system was introduced into our process. This system developed for laser cladding consists of two parts, E-MAqS and LompocPro. The E-MAqS monitors the melt pool area as soon as LMD process is started. Then the obtained pool area data are transferred to the Lompocpro and compared with the pool area setpoint. The laser power is controlled if these data can't correspond well to the pool area setpoint. The laser power will be decreased if these data are bigger than the pool area setpoint. On the contrary, it will be increased.

Figure 7(a) shows the pool area variations during multi-layer LMD process with water cooled substrate marked in blue and without water cooled substrate marked in red. The pool area during multi-layer LMD was measured on-line. It is increased more than 20% after 3000 seconds without water cooling of the substrate and has not reached a steady state yet. The heat accumulation effect is less when the substrate is cooled. The enlargement of the pool area can also be observed by comparing the images at the beginning (see Fig. 7(b)) and near the end (see Fig. 7(c)) of the process.

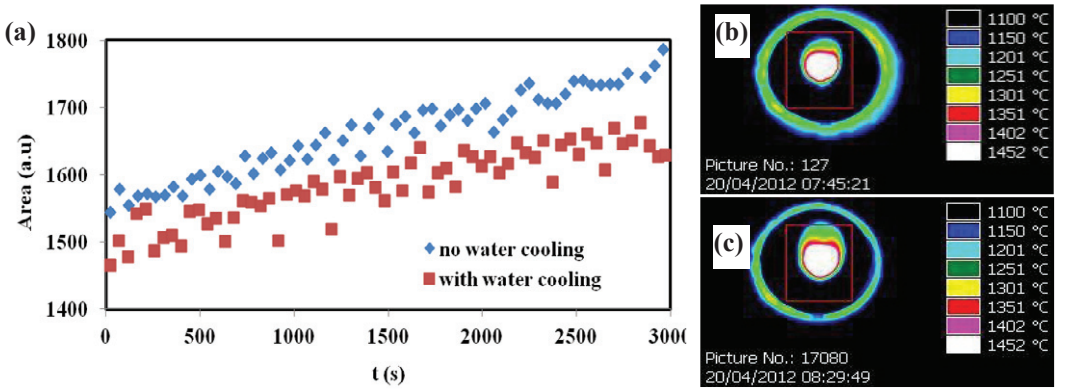

Fig. 7. Area variations during multi-layer LMD process using monitoring and control system ; (a) data analysis; (b) image at the beginning of the process; (c) image near the end of the process

In order to increase the deposition efficiency, a high scan speed is accepted as sets 4 and 5 in Table 1 wherein the other parameters are correspondingly changed to get a 0.5mm layer thickness. The interior qualities of the fabricated parts using both parameter sets wherein *P*=520W and *P*=570W, respectively, are good by further analyzing their cross sections (see Fig. 8(a)), which only have a few micro pores. The pool area was monitored and it kept increasing at the higher scan speed (Fig. 8(a)). The pool area has an increase of more or less 20% when using laser power 570W than using laser power 520W. This is much more than the increase of the laser power (~10%). Figure 8(b) shows the variations of the controlled laser power, changing according to the comparisons of the monitored pool area and the pool area setpoint. The current area setpoint, which is equal to 1950 and is provided according to the area level of using 570W laser power, was followed by the real pool area during the whole process by changing the laser power, even though the laser power dropped to a little lower than 500W due to the heat accumulation effect. The decreased heat inputs reduced the heat effect compared with the use of a constant 570W laser power during multi-layer deposition process. The interior quality of the fabricated part with controlled laser power is also good after checking its cross section, as shown in Fig. 8(b).

Macroscopic banding on the cross section of LMD Ti6Al4V parts, which has already been noted in several literatures [6, 12], is caused by the reheating of previously deposited material that occurred during the subsequent deposition process. This leads to microstructural changes like microstructural coarseness. Figure 9(a) shows this banding phenomenon clearly. The α' phase gets coarse and its aspect ratio is increased in region 1 compared to one in region 2 (see Figs. 9(1) and (2)). However, with control the overall cross section is more or less the same due to the decreased pool temperature and heat accumulation (see Fig. 9(b)). Besides, the total depth of the dilution and heat-affected zone of the substrate is decreased from 0.5mm to 0.35mm with the use of monitoring and control system, as illustrated in Figs. 9(a) and (b).

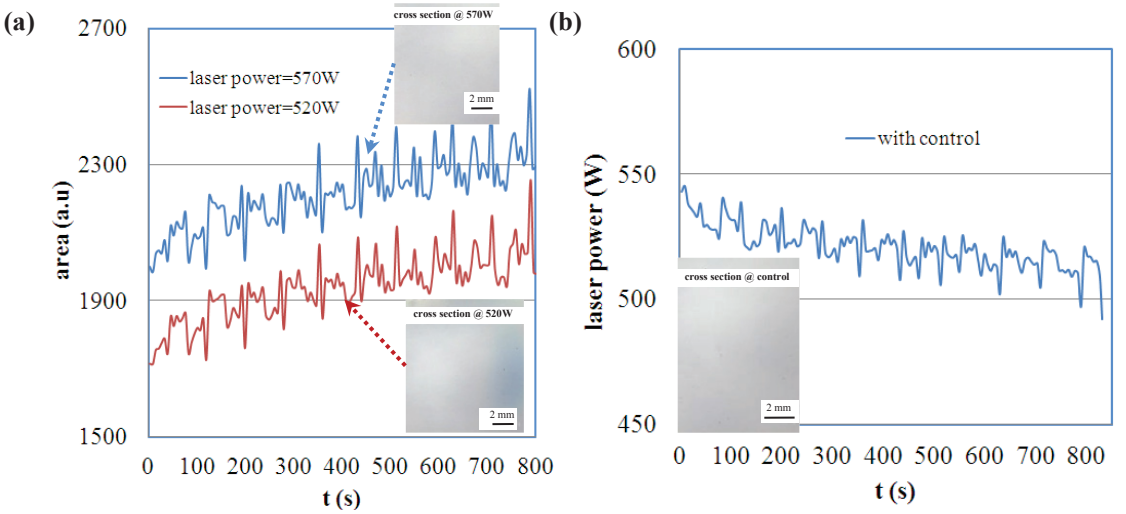

Fig. 8. Monitoring and control for LMD process using monitoring and control system; (a) area variations using parameter sets 4 and 5 in Table 1 with high scan speed; (b) variations of the controlled laser power with high scan speed (V=1500mm/min)

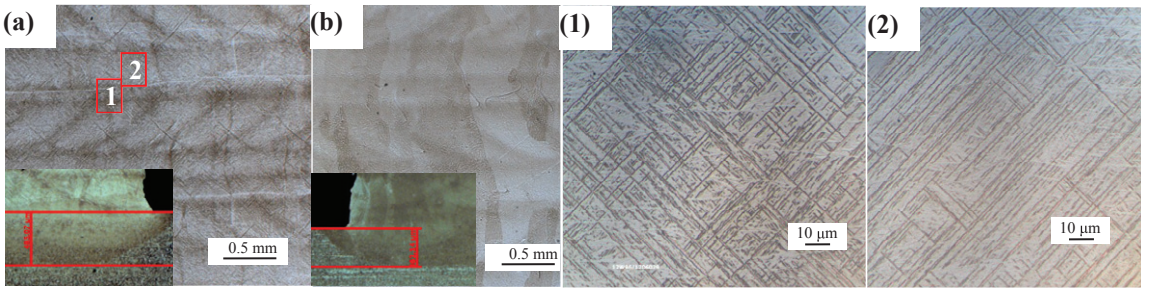

Fig. 9. Microstructures for specimens built without (a) and with (b) monitoring and control system (1) big magnification of region 1 (2) big magnification of region 2 in Fig. 9(a)

Conclusions

Based on the application requirements of laser metal deposition Ti6Al4V parts, the microstructure and mechanical properties of the fabricated parts were investigated. The microstructure shows typical acicular α'-martensite phase due to the rapid cooling of the melt pool. The hardness of the LMD parts is 360 ±10 HV and higher than the forging plate. The yield and ultimate tensile strengths are 976 ± 24 MPa and 1099 ± 2 MPa, respectively, which are superior to the cast and annealed wrought material. The elongation is lower (4.9 ± 0.1). These results depend on the formed microstructure and the minor elements content in the fabricated parts. The tested oxygen content was 0.13 wt% and can be decreased by the use of an inert gas chamber. Heat accumulation has much effect on the fabricated parts, like the microstructure, oxygen level, pool spreading behavior and heat distortion. The monitoring and control system was applied during LMD process to decrease the heat accumulation effect, by monitoring the pool area and controlling the laser power real-time. As a result, the microstructure is more or less consistent between layers and tracks and the total depth of the dilution and heat-affected zone is lowered as well.

References

[1] Arcella, F.; Abbott, D. H.; House, M. A.: Titanium Alloy Structures for Airframe Application by the Laser Forming Process. Alexandria: 2000: 1465-2000.

[2] Banerjee, R.; Collins, P. C.; Genc, A.: Direct Laser Deposition of in Situ Ti-6Al-4V-Tib Composites. Materials Science and Engineering A. 2003, 358: 343-349.

[3] Banerjee, R.; Nag, S.; Fraser, H. L.; A Novel Combinatorial Approach to the Development of Beta Titanium Alloys for Orthopaedic Implants. Materials Science and Engineering C. 2005, 25(3): 282-289.

[4] Rombouts, M.; Maes, G.; Persoons, R.: Material study of laser cladded Inconel 625. Material study of laser cladded Inconel 625. Innovative Developments in Virtual and Physical Prototyping, Proceedings of the 5th International Conference on Advanced Research in Virtual and Rapid Prototyping, Leiria, Portugal, 28 September - 1 October, 2011: 333-337.

[5] Thijs, L.; Verhaeghe, F.; Craeghs, T.; et al.: A study of the microstructural evolution during selective laser melting of Ti-6Al-4V. Acta Materialia 2010, 58: 3303-3312.

[6] Boyer, R.W.; Collings, G.E.W.: Materials properties handbook: titanium alloys. Materials Park (OH): ASM International; 1994.

[7] Murr, L.E.; Gaytan, S.M.; Medina, F.; et al.: Characterization of Ti-6Al-4V open cellular foams fabricated by additive manufacturing using electron beam melting. Mater. Sci. Eng. A 2010, 527, 1861-1868.

[8] Murr, L.E.; Esquivel, E.V.; Quinones, S.A.; et al.: Microstructures and mechanical properties of electron beam-rapid manufactured Ti-6Al-4V biomedical prototypes compared to wrought Ti-6Al-4V. Mater. Charact., 2009, 60: 96-105.

[9] Murr, L.E.; Quinones, S.A.; Gaytan, S.M.;et al.: Microstructure and mechanical behavior of Ti-6Al-4V produced by rapid-layer manufacturing, for biomedical applications. J. Mech. Behavior Biomed. Mater., 2009, 2: 20-32.

[10] Koike, M.; Greer, P.; Owen, K.; et al.: Evaluation of titanium alloys fabricated using rapid prototyping technologies-electron beam melting and laser beam melting. Materials 2011,4: 1776-1792.

[11] G. Lütjering. Influence of processing on microstructure and mechanical properties of (α+β) titanium alloys. Materials Science and Engineering A. 1998, 243: 32-45.

[12] Zhang, S. Y.: Research on the heat treated microstructures and properties of laser solid forming. Ph.D thesis of Northwest Polytechnical University. 2009.

[13] Kobryn, P.A.; Moore, E.H.; Semiatin, S.L.: The influence of laser power and traverse speed on microstructure, porosity, and build height in laser-deposited Ti-6Al-4V. Scripta mater. 43, 2000: 299-305.

[14] Fujii, H.: Nippon steel technical report, No. 62, July, 1994: 74-79.

[15] Eylon, D.; Newman, J. R.; Thorne, J. K.: Titanium and titaniun alloy casting. ASM Handbook, Volume 2, Properties and selection: nonferrous alloys and special-purpose materials, ASM International, 1990, in ASM Handbook on DVD, ASM International and The Dialog Corporation, 1999.2.

[16] Lampman, S.: Wrought titanium and titaniun alloy. ASM Handbook, Volume 2, Properties and selection: nonferrous alloys and special-purpose materials, ASM International, 1990, in ASM Handbook on DVD, ASM International and The Dialog Corporation, 1999.2.

[17] Zhou, Y. B.: Introduction to Titanium Alloy Casting. Beijing: Aviation Industry Press, 2000: 76-101.

[18] TAN S.S.: Non-ferrous metal materials. Beijing: Metallurgical Industry Press, 1993: 76-121.

[19] Tan, H; Chen, J; Zhang, F. Y; Lin, X.; Huang W. D.: Microstructure and Mechanical Properties of Laser Solid Formed Ti-6Al-4V from Blended Elemental Powders. Rare metal meterials and engineering, 2009, 38(4):0574-0578.

[20] Yu, J.; Lin, X.; Wang J.J.; et al.: Mechanics and energy analysis on melt pool spreading during laser solid forming. Applied Surface Science 2010, 256: 4612-4620.

[21] Huang, W.D.; Lin, X.; Chen, J.: Laser solid forming. Northwestern Polytechnical University Press. 1th Ed. Xi'an: 2007.4.